数理解析研究所講究録
第 774 巻 1991 年 126-138

Bifurcations in resonantly forced water waves

九大応力研 Mitsuaki Funakoshi（船越満明）
九大応力研 Susumu Inoue（井上 進）

Abstract. Water waves are generated when a container halfly filled with a fluid is oscillated sinusoidally in a horizontal direction. For the resonant case in which a forcing period T is close to the natural period of two degenerate modes, Miles derived a nonlinear equation for four variables related to the modulations of these modes. We examine the T-dependence of solutions to this equation within the parametric region of no stable fixed point for several values of forcing amplitude x_0 and damping coefficient α. Based on the computations of periodic orbits (of period τ), we find that, when x_0 increases with α fixed or when α decreases with x_0 fixed, the T-dependence becomes more complicated owing to the generation of new branches of periodic orbit through homoclinic bifurcation, appearances of folds and kinks in the τ-T curve of each branch, merging of branches, and destabilization of periodic orbits by period-doubling and symmetry-breaking bifurcations.

1. Introduction

Water waves are generated when a cylindrical container filled with a fluid up to the depth d and of radius a is oscillated horizontally in one direction. The eigenmodes of these waves are generally written as $\eta = (A_1(t)\cos m\theta + A_2(t)\sin m\theta)J_m(k_{m,n}r)$ for the free-surface displacement $z = \eta$. Here z is the vertical upward coordinate, and (r, θ) plane polar coordinates on which the axis of oscillation is $\theta = 0$ and π. Positive integer n is defined so that $k_{m,n}a$ is the n-th positive zero of J'_m, while m is a circumferential wavenumber. In the (m, n) mode, $A_1(t)$ and $A_2(t)$ change sinusoidally with the natural frequency $\omega_{m,n}$.

We study the resonant case in which the displacement of the container is expressed as $x = x_0\cos(2\pi t/T)$ and the forcing period T is close to the natural period $T_0(= 2\pi/\omega_{1,1})$ of two degenerate (1,1) modes. Here $\omega_{1,1} = \sqrt{g k_{1,1} \tanh k_{1,1} d}$ (g : gravitational acceleration). Then η can be approximately written as

$$\eta = a[(p_1 \cos \omega t + q_1 \sin \omega t) \cos \theta + (p_2 \cos \omega t + q_2 \sin \omega t) \sin \theta] J_1(kr) \ . \tag{1}$$

Here $\omega = 2\pi/T$, $k = k_{1,1} = 1.8412/a$, and four variables p_1 , q_1 , p_2 , and q_2 can change with the time scale much larger than T. In order to analyse this resonant case, [Miles, 1984] assumed that

$$\left.\begin{array}{l} \varepsilon \equiv (x_0/a)^{1/3} \ll 1, \qquad p_n, q_n = O(\varepsilon), \quad [n = 1,2], \\ \text{(time scale of the changes of } p_n \text{ and } q_n)/T = O(\varepsilon^{-2}), \\ T_r \equiv (T - T_0)/T_0 = O(\varepsilon^2), \end{array}\right\} \tag{2}$$

and derived the following nonlinear equations for p_n and q_n

$$\left\{\begin{array}{l} \dot{p}_1 = -\alpha p_1 - (\beta + AE) q_1 + BM p_2 \ , \\ \dot{q}_1 = -\alpha q_1 + (\beta + AE) p_1 + BM q_2 + c x_0/a \ , \\ \dot{p}_2 = -\alpha p_2 - (\beta + AE) q_2 - BM p_1 \ , \\ \dot{q}_2 = -\alpha q_2 + (\beta + AE) p_2 - BM q_1 \ , \end{array}\right. \tag{3}$$

under the assumptions of weak nonlinearity and linear damping of $O(\varepsilon^2)$. Here dotts denote the derivative with respect to $t'(= \omega t)$. Since $M = p_1 q_2 - p_2 q_1$ and $E = ({p_1}^2 + {q_1}^2 + {p_2}^2 + {q_2}^2)/2$, the terms including M or E are nonlinear ones of third-order. The parameter β, given by $\beta = (\omega^2 - \omega_{1,1}^2)/2\omega_{1,1}^2$, corresponds to the difference between the natural frequency (period) and the forcing frequency (period). We hereafter use T_r defined in (2) in place of β to express this difference. Also α is a coefficient of linear damping. The values of coefficients A, B, and c depend only on a/d. [Miles,1984] found that (3) has periodic and chaotic solutions as well as fixed points. In this paper, we examine the dependences of the solutions to (3) on parameters $x_0/a, \alpha$, and T_r in detail. Here we used the values $A = 0.224$, $B = -0.306$, $c = 1.315$, which correspond to $a/d = 0.655$.

2. Solutions to equation (3)

Equation (3) has the property that if $(p_1(t') \, , q_1(t') \, , p_2(t') \, , q_2(t'))$ is a solution to (3) for parameters α , x_0/a , β , A , B , and c, then for any positive value ν , $(\nu p_1(\nu^{-2} t') \, , \nu q_1(\nu^{-2} t') \, ,$

$\nu p_2(\nu^{-2}t')$, $\nu q_2(\nu^{-2}t'))$ is the solution for parameters $\nu^2\alpha$, $\nu^3 x_0/a$, $\nu^2\beta$, A , B , and c. Therefore, we can obtain essentially the same solution for all sets of values of $(x_0/a\ ,\alpha)$ satisfying the condition $\alpha/(x_0/a)^{2/3} = const.$ under the appropriate transform of the value of T_r. Therefore, we hereafter fix the value of α to 0.0043 and examine the T_r-dependence of the solution for several x_0/a .

Fixed points of (3) are composed of a one-dimensional mode in which only $\cos\theta$ mode is excited ($p_2 = q_2 = 0$) and a rotational mode in which both $\cos\theta$ and $\sin\theta$ modes are excited and the point of largest η rotates in a definite direction [M, 1984] . Figure 1 shows a typical T_r-dependence of fixed points. Supercritical Hopf bifurcations (hereafter referred to as H.b.'s) of the rotational mode occurs at two points A and B. Since this mode is unstable between these points, there is no stable fixed point in the T_r region between A and C, a turning point of the one-dimensional mode. For sufficiently small x_0, however, since the H.b. does not occur, at least one stable fixed point exists for all T_r. These results are summarized in Fig.2, where no stable fixed point exists in a hatched region. We mainly examine the solutions for parameters in this region.

We first computed a series of attractors for a few fixed values of x_0 by slowly increasing T_r from the value a little smaller than the left edge of the above parametric region. For each attractors, we computed the set S of values taken by M when the orbit intersects a hyperplane $p_1 =< p_1 >$. Here $< p_1 >$ is the average value of p_1. For fairly small x_0, within wide regions of T_r, S is composed of few points, corresponding to the limit cycles which express periodic modulations of water waves (see Fig.3(a)). And only in few relatively narrow regions of T_r, we find chaotic attractors in which S is composed of many points and which correspond to irregular modulations of water waves. For large x_0, however, chaotic attractors are found more commonly, and limit cycles exist in many narrow windows, as shown in Fig.3(b). The alternation between limit cycles and chaotic attractors is frequent for large x_0. Therefore, the T_r-dependence of the attractors becomes more complicated with the increase of x_0. Furthermore, we find the following variations of the T_r-dependence of limit cycles caused by the increase of x_0 : (i) A limit cycle revealing continuous T_r-dependence loses the continuity at a certain x_0. (ii) The T_r region where a limit cycle exists with the continuous T_r-dependence extends abruptly at a certain x_0.

3. Periodic orbits

Aiming at resolving the process to more complicated T_r-dependence of the attractors associated with the increase of x_0, we computed, as the first step, periodic orbits of (3) with a kind of Newton method, almost the same as those introduced in [Sparrow, 1982]. The periodic orbits are classified into a unidirectional periodic orbit (hereafter referred to as u.p.o.) and a bidirectional periodic orbit (b.p.o.). Here u.p.o., corresponding to the unidirectional rotation of the point of largest η of water waves, yields the M values of definite sign almost all time. On the contrary, M for b.p.o. takes both positive and negative values, expressing the alternations of clockwise and anticlockwise rotations of water waves. Furthermore, b.p.o. is composed of symmetric and asymmetric ones, only the former of which is invariant with respect to the transformation $(p_1, q_1, p_2, q_2) \to (p_1, q_1, -p_2, -q_2)$. We mainly examine the symmetric ones.

Stable fixed points exist for all T_r only if x_0 is less than $0.00103a$, as shown in Fig.2. Period τ of periodic orbits for x_0 a little larger than this value is shown in Fig.4(a). We find an approximately straight branch of stable u.p.o. connecting H_1 and H_2, the H.b. points of the rotational mode. With the increase of x_0, a part of large τ appears on this branch, as shown in Fig.4(b), and then the separation of the u.p.o. branch associated with the appearance of a symmetric b.p.o. branch is found, as shown in Fig.4(c). Here and hereafter half the period is expressed for b.p.o.'s in figures. At the boundaries of these branches, τ tends to infinity indicating the existence of homoclinic orbits associated with the fixed point of the one-dimensional mode. This kind of homoclinic bifurcation (hereafter referred to as h.b.) occurs also for larger x_0. In Fig.5, we can see five branches resulting from the separation of the b.p.o. branch in Fig.4(c) associated with the appearance of a new u.p.o. branch. These h.b.'s are summarized in Fig.6. Here solid lines denote the parameter values for homoclinic orbits excepting that the lowest solid line is the H.b. point of the rotational mode. It can be roughly said that in each region surrounded by these lines, each u.p.o. or b.p.o. branch exists.

The behaviour of the τ-T_r curve when τ tends to infinity is classified into two types. In type I, T_r increases or decreases monotonically as $\tau \rightarrow \infty$, while T_r oscillates with decreasing amplitude in type II. In Fig.6, crosses and circles denote type I and II, respectively. [Glendinning and Sparrow, 1984] examined a three-dimensional system containing a homoclinic orbit associated with a fixed point of saddle-focus type with eigenvalues $\nu_1(> 0)$ and $\nu_2 \pm i\omega_2$ ($\nu_2 < 0$). According to a local analysis, they showed that type I and II are obtained when $|\nu_2|/\nu_1$ is larger and smaller than one, respectively. The eigenvalues of the fixed point related to the homoclinic orbits in our four-dimensional system (3) have the same properties as the above eigenvalues except for the addition of the fourth one $\nu_3(< 0)$. The computed value of $|\nu_2|/\nu_1$ in (3) is smaller than one in the region above the doubly-dotted broken line in Fig.6. Therefore, the types of the τ-T_r curve in (3) can be explained well based on the result of above analysis. This is probably because $|\nu_3|/|\nu_2|$ is so large that the fourth dimension can be approximately neglected.

We call the u.p.o. branch starting from the lower H.b. point as branch I, and the next b.p.o. branch as branch II. We examine these branches in detail. The orbit in branch I is stable for all T_r if x_0 is small enough not to undergo the h.b., as shown in Figs.4(a) and (b). At x_0 close to the value of the first h.b., a fold of the τ-T_r curve of this branch appears, as shown in Fig.4(c), and discontinuous T_r-dependence of limit cycles and histeresis are observed. For larger x_0, a stable region of this branch becomes unstable through a pair of supercritical period-doubling bifurcations (hereafter referred to as p.d.b.'s), as shown in Fig.7(a). The attractors in this destabilized region become more complicated through successive p.d.b.'s as T_r goes farther from the points of the first p.d.b. When the width of this region is sufficiently large, chaotic attractors appear at the central part of this region. One typical example is shown in the region $0.0065 \leq T_r \leq 0.0095$ of Fig.3(a). Next at

$x_0 = 0.00224a$, a new u.p.o. branch (referred to as branch I^+) emerges as a small closed τ-T_r curve, whose size then becomes larger as x_0 increases. Branches I and I^+, which are separated in Fig.7(b), merge at $x_0 = 0.002294a$, as shown in Fig.7(c). Consequently, when T_r is decreased from points A in Figs.7(b) and (c), the relevant limit cycle exists continuously only until $T_r = 0.0102$ in (b), while until $T_r = 0.0088$ in (c). That is, the T_r region where the limit cycle exists continuously extends abruptly owing to the merging of two branches. As x_0 increases further, the τ-T_r curves in Figs.7 (d)-(f) reveal more complicated winding through the appearance of folds and the merging with other branches. For example, a new branch appeared at $x_0 = 0.00344a$, illustrated in Fig.7(e), merges with branch I, as shown in Fig.7(f). Moreover, the width of unstable regions emerged through p.d.b.'s becomes larger as x_0 increases, resulting in the contraction of stable regions to narrow windows.

Periodic orbits in branch II are stable for all T_r just after its appearance through h.b. at $x_0 = 0.001195a$, as shown in Fig.4(c). Similarly to the case of branch I, a fold appears as x_0 increases (see Fig.5). Moreover, a stable region of this branch becomes unstable through a pair of symmetry-breaking bifurcations (hereafter referred to as s.b.b.'s), as illustrated in Figs.5 and 8(a). Near the both ends of the destabilized region, asymmetric b.p.o.'s are obtained as attractors. Furthermore, successive p.d.b.'s of these b.p.o.'s and chaotic attractors are found when the width of this region is sufficiently large. If x_0 increases further, a kink appears in a part of the τ-T_r curve, as found in Fig.8(c), resulting in discontinuous T_r-dependence and the occurence of histeresis of the limit cycle. At $x_0 = 0.00244a$, a new branch called as branch II^+ emerges. Branches II and II^+, separated in Fig.8(c), merge at $x_0 = 0.002483a$, as found in Fig.8(d). (The intersection of the τ-T_r curves of these branches in Fig.8(c) does not mean the connection of them.) Therefore, the abrupt change of the T_r region where the limit cycles decreasing from B in Figs.8(c) and (d) exist continuously occurs. For larger x_0, further appearances of kinks and folds and occurences of s.b.b.'s give rise to the state of many narrow windows of stable periodic orbits (see Figs.8(e) and (f)).

4. Conclusions

Based on the computations of periodic orbits of (3) in the parametric region of no stable fixed point, we found that, when x_0 increases with α fixed, the T_r-dependence of the solutions to (3) becomes more complicated owing to the generation of new branches of periodic orbit through h.b., appearances of folds and kinks in the τ-T_r curve of each branch, merging of branches, and destabilization of periodic orbits by p.d.b.'s and s.b.b.'s. According to the property of (3) mentioned in section 2, this complication of the T_r-dependence occurs also when α decreases with x_0 fixed.

We acknowledge the technical assistance of Miss Hoshino.

REFERENCES

Glendinning,P.and Sparrow,C.,1984,Local and Global Behavior near Homoclinic Orbits, *J.Stat.Phys.*,**35**,645-696.

Miles,J.W., 1984, Resonantly Forced Surface Waves in a Circular Cylinder,*J.Fluid Mech.*, **149**,15-31.

Sparrow,C.,1982, *The Lorenz Equations : Bifurcations,Chaos, and Strange Attractors*, Springer-Verlag,New York.

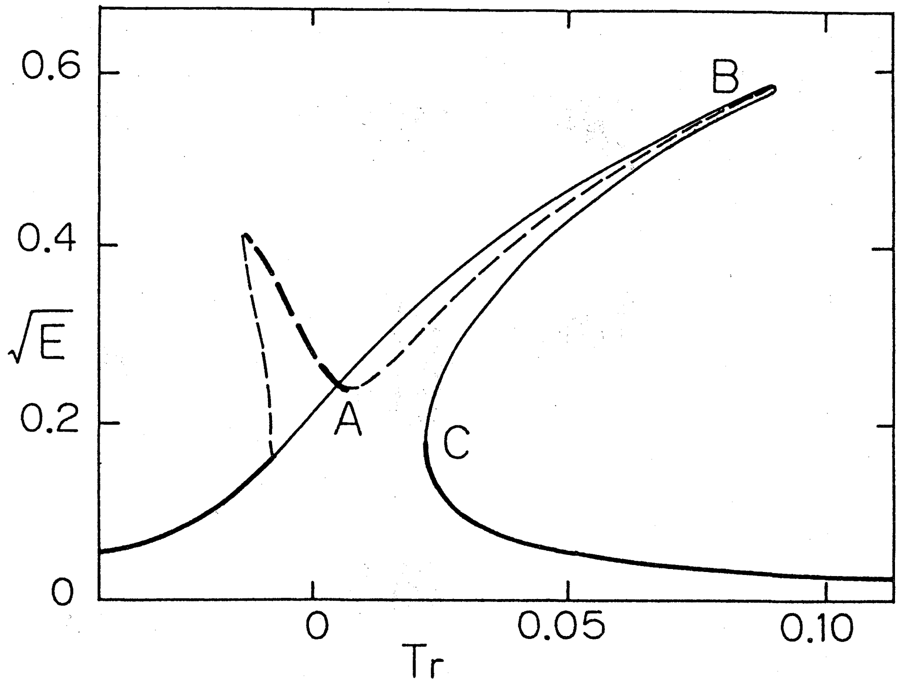

Fig.1 Typical T_r-dependence of fixed points. Solid line denotes the one-dimensional mode, and broken line the rotational mode. Bold and thin lines express stable and unstable fixed points,respectively. x_0=0.002706a.

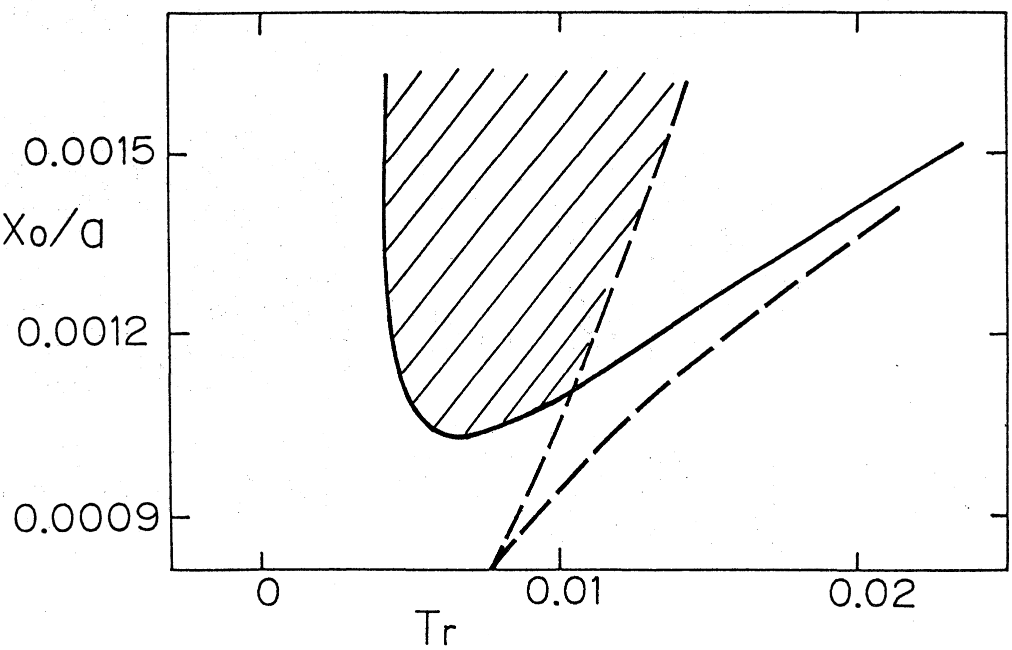

Fig.2 Bifurcation points of fixed point. Solid line denotes the H.b. point of the rotational mode, and broken line the turning point of the one-dimensional mode.

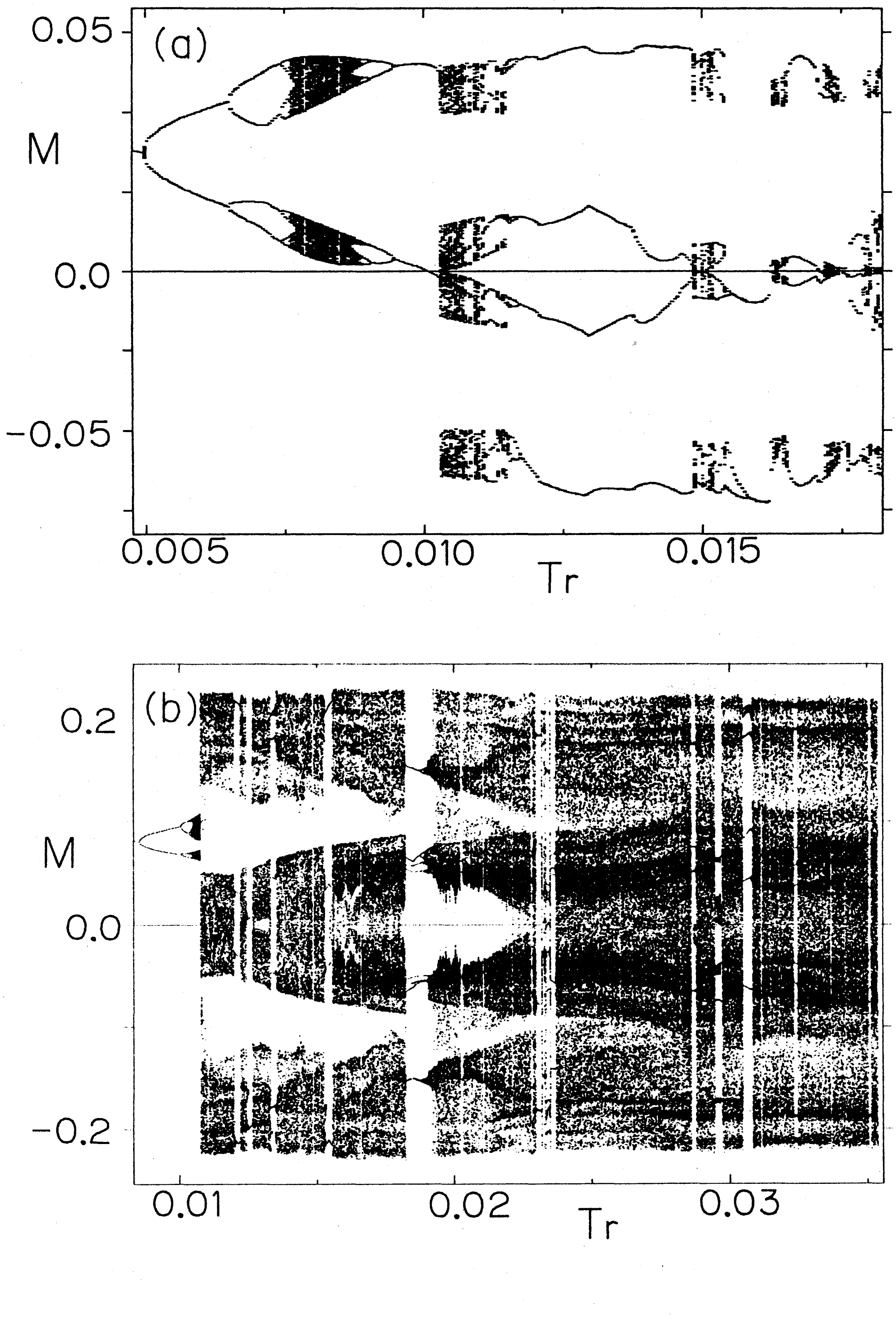

Fig.3 T_r-dependence of attractors. (a) x_0=0.002165a, (b) 0.005411a.

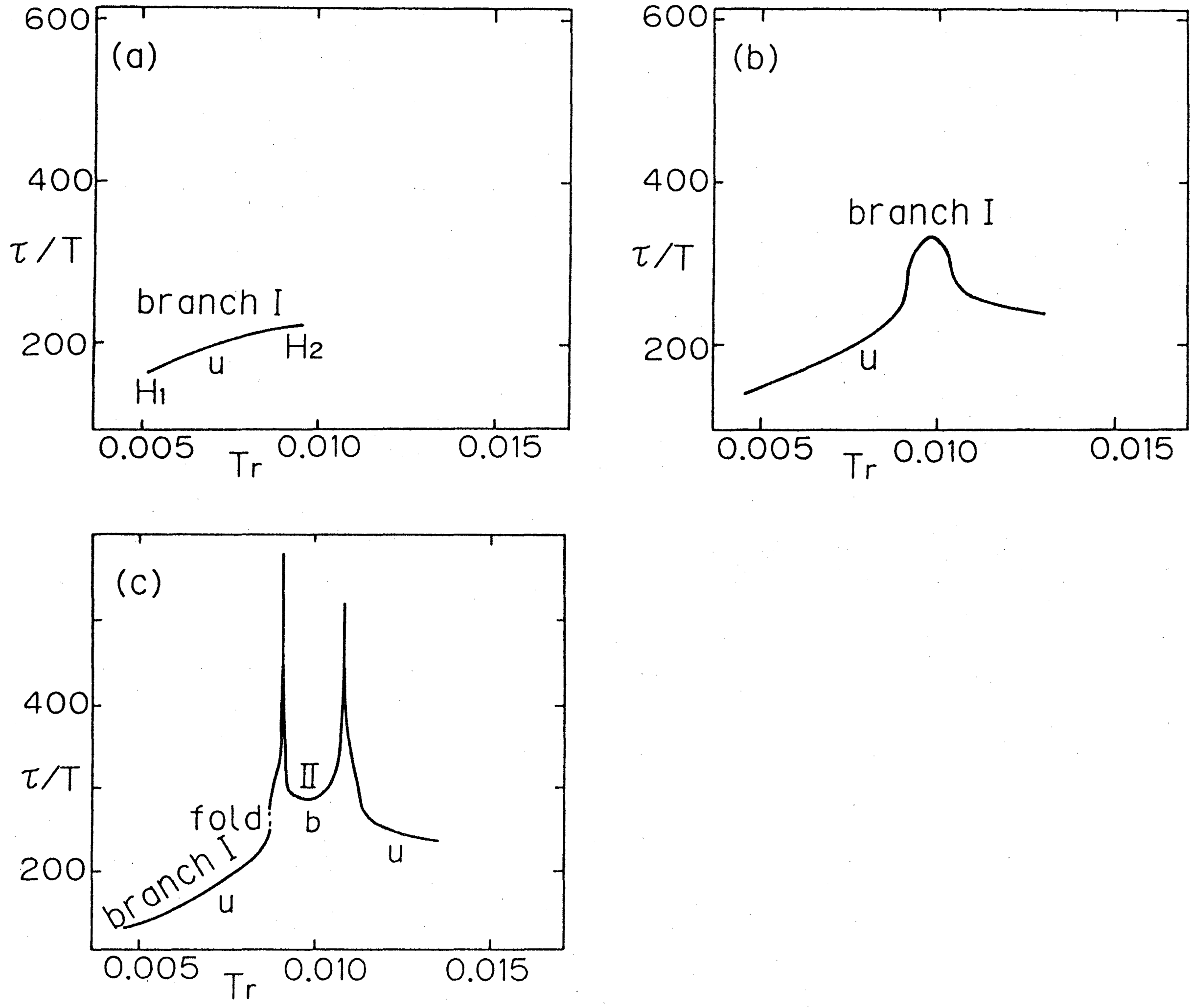

Fig.4 T_r-dependence of periodic orbits. Solid and broken lines denote stable and unstable periodic orbits, respectively. u.p.o. and b.p.o. branches are expressed by u and b, respectively. (a) $x_0/a = 0.001082$, (b) 0.001190, (c) 0.001201.

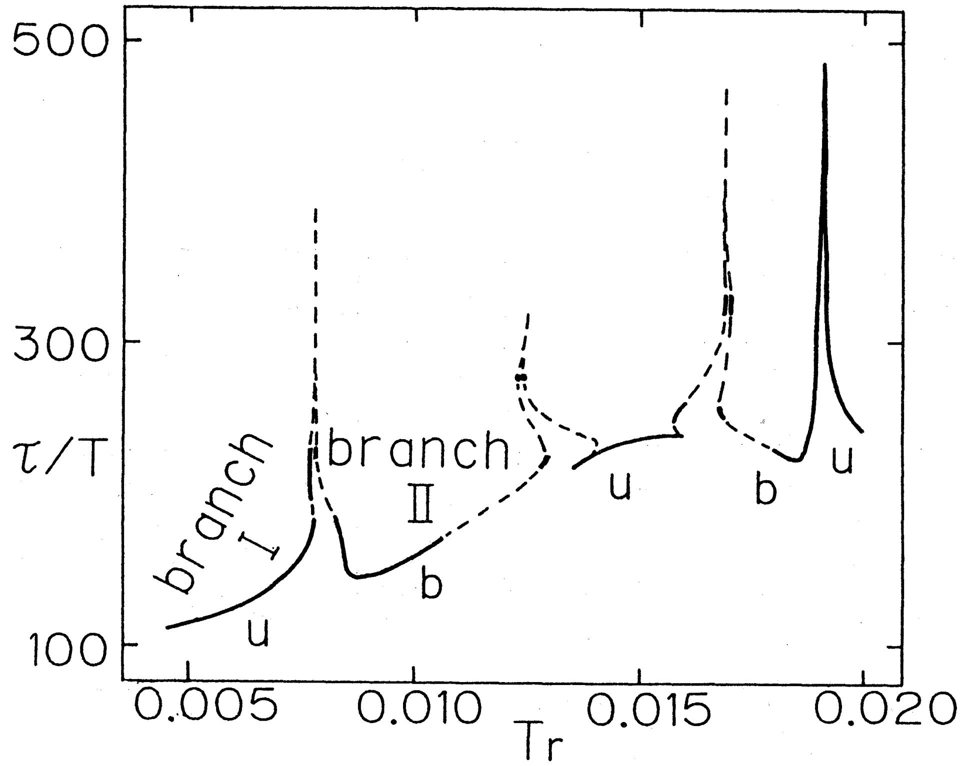

Fig.5 T_r-dependence of periodic orbits. Same symbols as in Fig.4 are used. $x_0/a = 0.001407$.

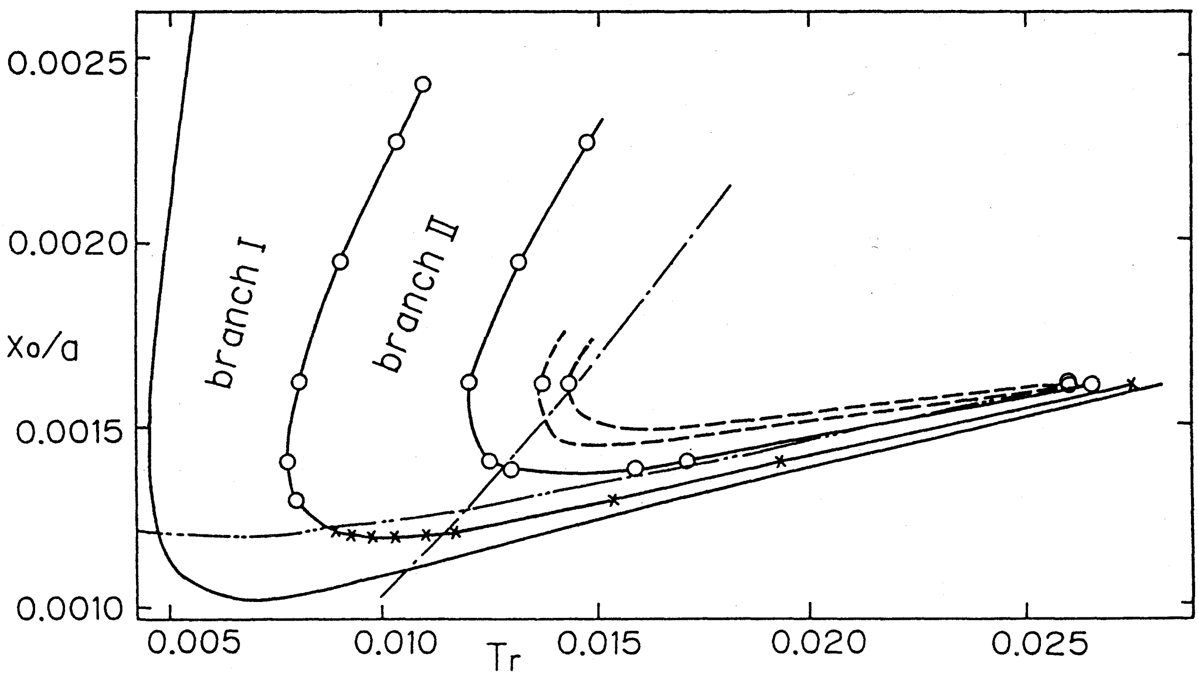

Fig.6 Parameter values for homoclinic orbits are expressed by solid lines (inferred values are shown by broken lines). Dotted-broken line denotes the turning point of the one-dimensional mode.

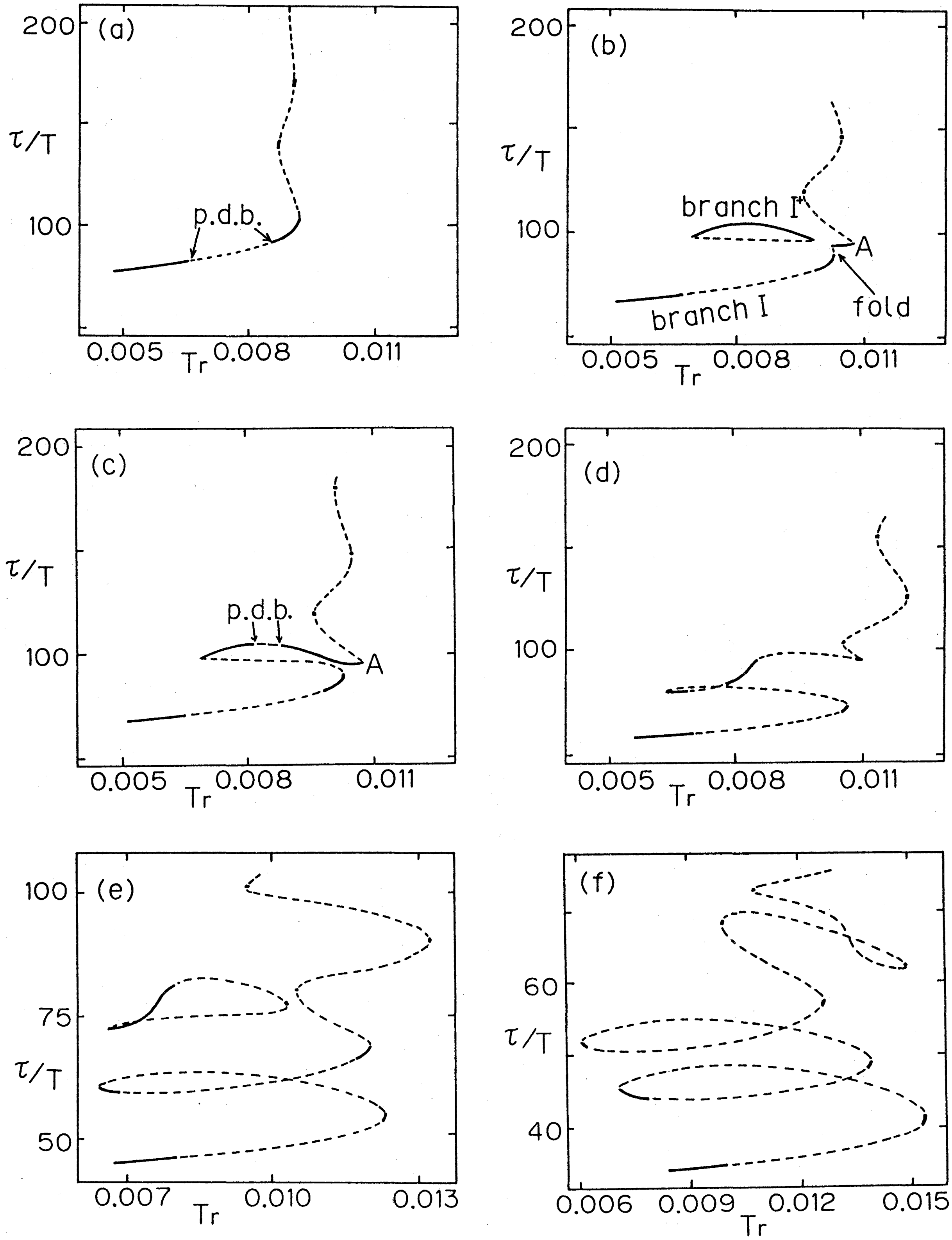

Fig.7 T_r-dependence of u.p.o. of branch I. Same symbols as in Fig.4 are used. (a) x_0/a = 0.001948, (b) 0.002289, (c) 0.002294, (d) 0.002706, (e) 0.003680, (f) 0.005411.

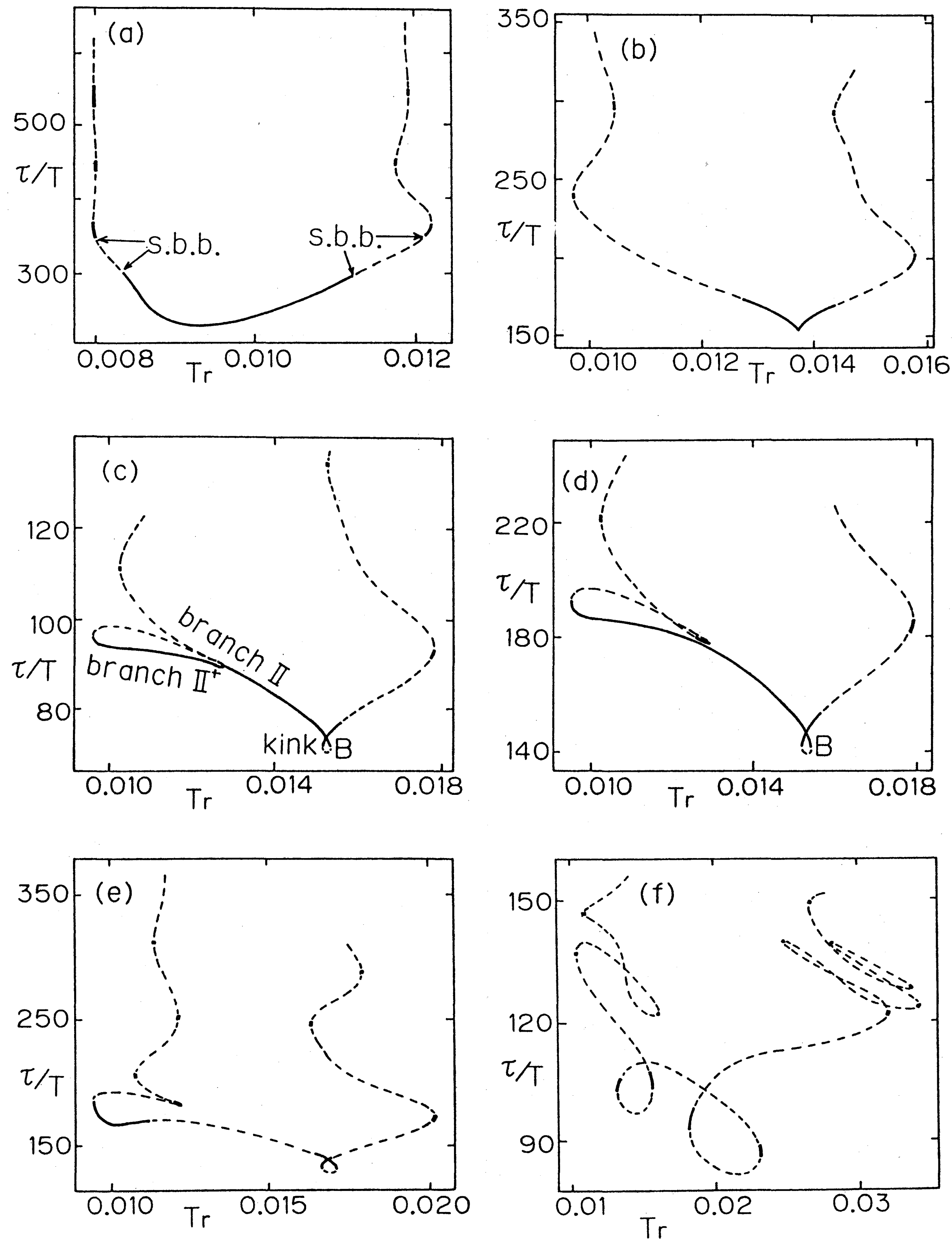

Fig.8 T_r-dependence of b.p.o. of branch II. Same symbols as in Fig.4 are used. (a) x_0/a = 0.001623, (b) 0.002273, (c) 0.002478, (d) 0.002489, (e) 0.002706, (f) 0.005411.